

Structural and Electrical Studies of PVP and PVDF Based Blend Polymer Electrolytes

Raju vaddiraju¹, M.Vinoda rani², Malla Reddy Yalla³, Venkata Ramana Jeedi⁴, A. Sadananda chary⁵, S. Narender Reddy^{6*}

¹Vignan's Institute of Management and Technology for Women, kondapur, Ghatkesar, Hyderabad, 501301, Telangana, India

²Department of Physics, University College of Science, Osmania University, Hyderabad-500007, Telangana, India

³Department of Physics, University PG College, Osmania University, Secunderabad, Hyderabad, Telangana, India

⁴Department of Physics, B.V Raju Institute of Technology, Narsapur, Medak Dist, 502313, India

⁵Department of Physics, Jawaharlal Nehru Technological University, Hyderabad-500085, Telangana, India

⁶Department of Physics, Jawaharlal Nehru Technological University, Hyderabad-500085, Telangana, India

Abstract: Poly (vinylpyrrolidone) (PVP) and Poly (vinylidene fluoride) (PVDF) have been used as copolymers and NaClO₄ as salt to prepare solid polymer blend electrolyte systems by using solution cast method. X-ray diffractogram, Fourier Transform Infrared Spectroscopy and Scanning Electron Microscopy studies confirm the complexation of salt with polymer blend. PVP and PVdF weight percentages are varying while maintaining a constant weight % of NaClO₄. AC and DC conductivity studies are carried out for all blend systems. Impedance spectroscopy has been used to examine the dielectric properties and electric modulus (M^*) in the frequency range 10Hz-30 MHz for all the systems. The maximum ionic conductivity $9.334 \times 10^{-5} \text{ Scm}^{-1}$ was noticed for PVP: PVDF: NaClO₄ (80:20:16) system at room temperature, which implies that decrease in crystallinity and increase in amorphous phase formation. Ionic conductivity of all the blend systems were increased with temperature according to Arrhenius behaviour.

Keywords: Solution cast method, Blend polymer electrolyte, SEM, FTIR, XRD, Impedance analysis, Nyquist plots.

1. Introduction:

SPEs have a significant technological role in the production of super capacitors, fuel cells, batteries, smart windows and sensing equipment [1-2]. These provide a number of benefits over liquid electrolytes namely safe operation, greater equipment life, the avoidance of electrolyte leaks and electrochemical stability over wide operating temperature range [3-4]. X-ray diffraction (XRD) and Fourier transform infrared (FTIR) spectroscopy revealed the complexation of NaClO₄ salt with the mixture of polymers PVP and PVDF. Differential scanning calorimetry was used to determine the melting temperatures (DSC). Scanning electron microscopy was used to analyse the surface morphology (SEM).

Electrical impedance spectroscopy (EIS) was used to examine the produced films in order to explore ionic conductivity, dielectric properties and electrical modulus properties. The SPE films have a number of properties including thermal, mechanical, electrochemical stability and flexibility. An alkaline metal or alkali metal salt is dissolved in a host polymer to create these SPEs [5-7].

2. Experimental procedure

Sodium perchlorate (NaClO₄, AR, >=98.0%), Poly (vinylpyrrolidone) (PVP, Mw = 3,60,000), and poly (vinylidene fluoride) (PVDF, Mw = 2,75,000) were acquired from Sigma Aldrich, India, Merck furnished the dimethyl formamide (DMF, AR grade). The Salt concentration has been varied with fixed blend composition (80PVP/20PVDF/xwt%NaClO₄ where, x=4, 8, 12, 16 and 20). In these systems, the ionic conductivity rises with NaClO₄ upto 16wt% and there after decreases. The highest ionic conductivity has been observed for PPN-16 system (80 PVP / 20 PVDF / 16 NaClO₄) which exhibits a highly amorphous nature.

3. Results and Discussion

3.1 XRD studies

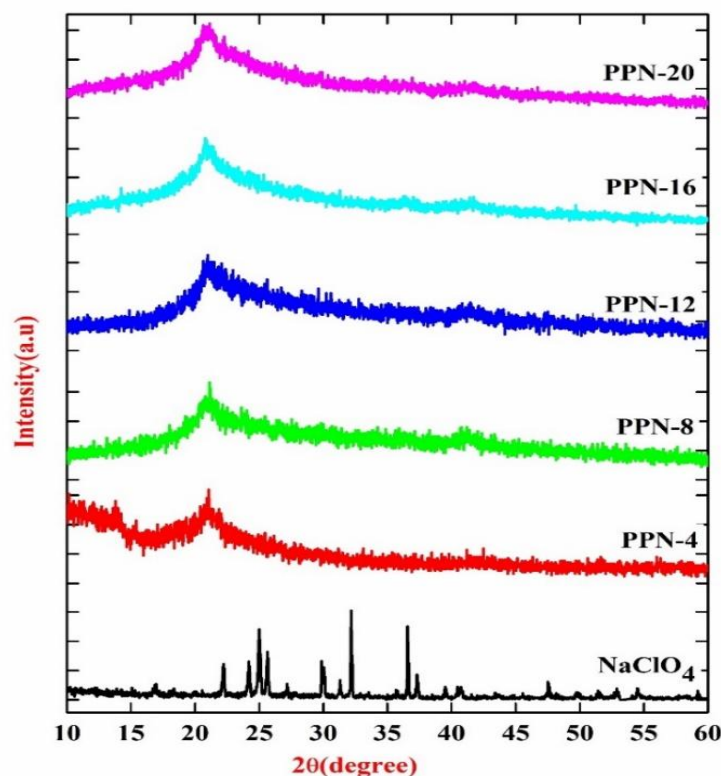


Fig. 3.1 X-ray diffraction patterns of pure NaClO_4 and blend polymer electrolytes.

Fig. 3.1 shows the X-ray Diffraction patterns of Pure NaClO_4 and various weight percentages of NaClO_4 Complexed blend compact polymer electrolytes (CSPE). The disappearance of the individual peak of NaClO_4 at 32.5° in all systems is evidence of the salt complex in all these electrolyte systems, the uncomplexed PVP peaks at 19° and 22° in all PPN-electrolyte systems. The presence of wider peaks at 38.9° and 20.22° indicates the semicrystalline characteristics of the α and β phases of PVDF respectively [1,8]. As varying content of NaClO_4 (up to 4wt%) were added to the blend polymer electrolyte system, it was observed that the interaction between salt (NaClO_4) particles and the host polymer matrix, the peak broadening increased and shifted towards shorter angles. The electrolyte systems of the host polymers might undergo structural reformation. [9].

Table: 3.1 Sample code, composition ratio, XRD parameters of several complexed solid polymer electrolyte systems

Sample Code	PVP: PVDF: NaClO_4	2θ (Degree)	FWHM (Degree)
PPN-4	80:20:04	20.78	1.95
PPN-8	80:20:08	21.01	1.78
PPN-12	80:20:12	21.16	1.95
PPN-16	80:20:16	20.75	2.20
PPN-20	80:20:20	21.04	1.68

3.2 Scanning Electron Microscopy

Figure 3.2 displays SEM images of complexed blend polymer electrolytes. Figure 3.2(a) depicts the blend polymer electrolyte PPN-4 system. Figure 3.2(b-e) shows complexed systems of PPN-8, PPN-12, PPN-16, and PPN-20 individually. The dissimilar sized spherulites found in all PPN-systems, in addition to the spherulites there are also amorphous regions. The amorphous areas of polymer blend systems increases as NaClO_4

concentration increases, whereas spherulitic regions decreases[2].With increasing salt content, this proves that decreased crystallinity and increased amorphous nature, Spherulite area disappeared entirely at 4wt% of NaClO_4 salt when diffrentiate to other electrolyte systems.The PPN-16 electrolyte system displays the greatest degree of homogeneity.

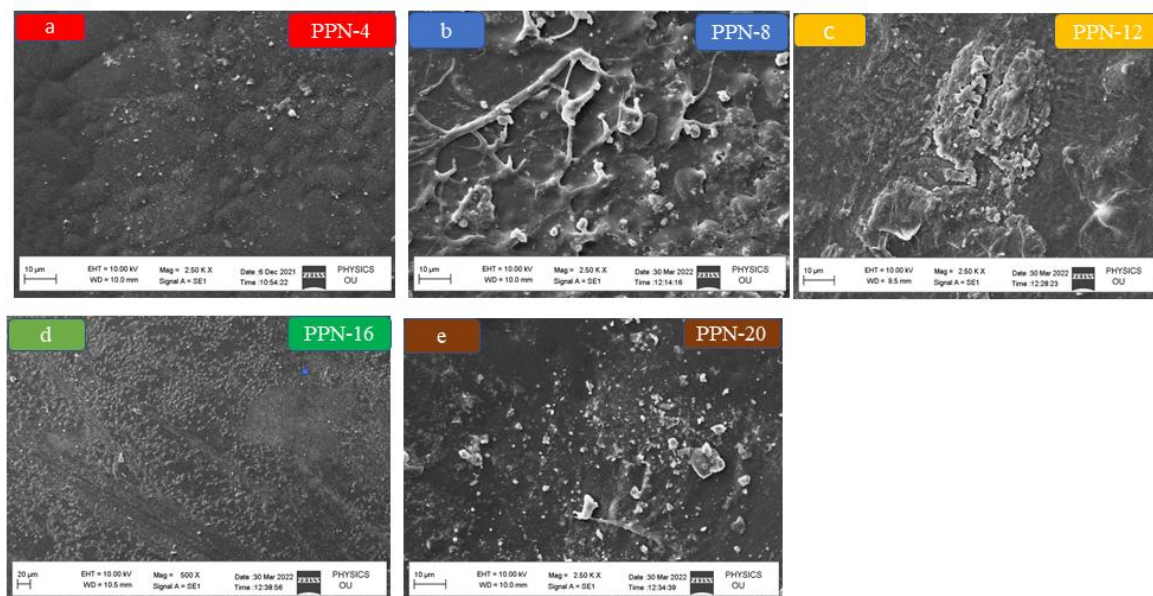


Fig. 3.2. SEM morphological pictures of (a) PPN-4 (b) PPN-8 (c) PPN-12 (d) PPN-16 and (e) PPN-20

3.3D.C Conductivity

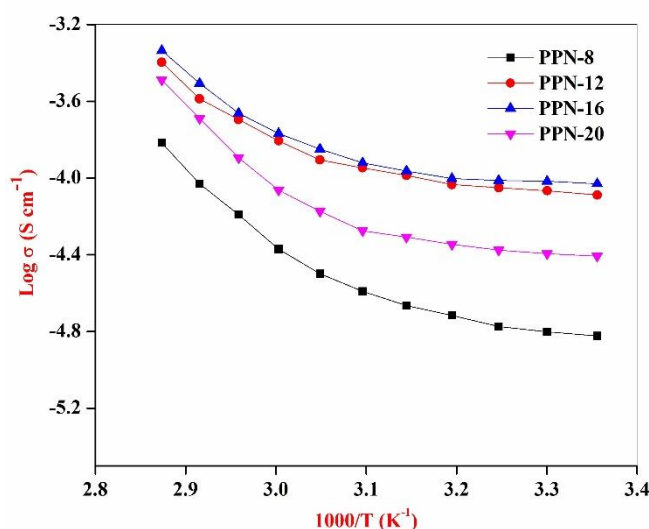


Fig. 3.3 Arrhenius plot: Variation of $\text{Log } \sigma$ Vs $1000/T$

The D.C ionic conductivity of each CSPE system is determined and displayed in table. 3.3 The conductivity with inverse temperature plots for every PPN systems has been displayed in fig.3.3 It has been perceived that the D.C conductivity increases up to 16wt% of salt content and then decreases. The addition of more salt leads to the creation of ion pairs and ion clusters, which in turn limit the mobility of ionic and polymeric segments [10, 11]. The activation energy (E_a) can be obtained in table 3.3.1 and was calculated from the slopes of the $\text{log } \sigma$ vs. $1000/T$ plot. It can be noticed that PPN-16 system possesses the least activation energy (E_a) which corresponds to maximum ionic conductivity compare to all other systems. The ionic transport number at 298K was calculated for all systems using Wagner's polarization technique and is shown in table 3.3.1.

Table: 3.3.1 Sample code, activation energy, ionic conductivity and ion transport number of various complexed solid polymer electrolyte systems

Sample Code	Activation energy E_a (eV)	Ionic conductivity (S.cm ⁻¹)	Ion transport number (T_{ion})
PPN-8	0.533	1.502×10^{-5}	0.81
PPN-12	0.523	8.164×10^{-5}	0.88
PPN-16	0.514	9.334×10^{-5}	0.90
PPN-20	0.529	3.918×10^{-5}	0.86

3.4 Electrical impedance studies

3.4.1 Real Electric Modulus

3.4.1 (a) shows the real electric modulus (M') exhibits frequency dependence for all PPN systems at room temperature. M' of all systems shifts to high frequency by increasing NaClO_4 concentration up to 16 wt%. All PPN systems have been observed constant M' values reach until 10^5 Hz, and then to become nonlinear between 10^5 Hz to 10 MHz in the high-frequency range. Figures 3.4.1 (b-f) show the temperature dependence of PPN-4, PPN-8, PPN-12, PPN-16, and PPN-20 individually. It is clear from the graphs that when the temperature increases, the M' dispersion moves towards its highest frequency. The abrupt change in M' not only indicates the absence of electrode interface polarization but also signals the onset of the hopping mechanism [12-13].

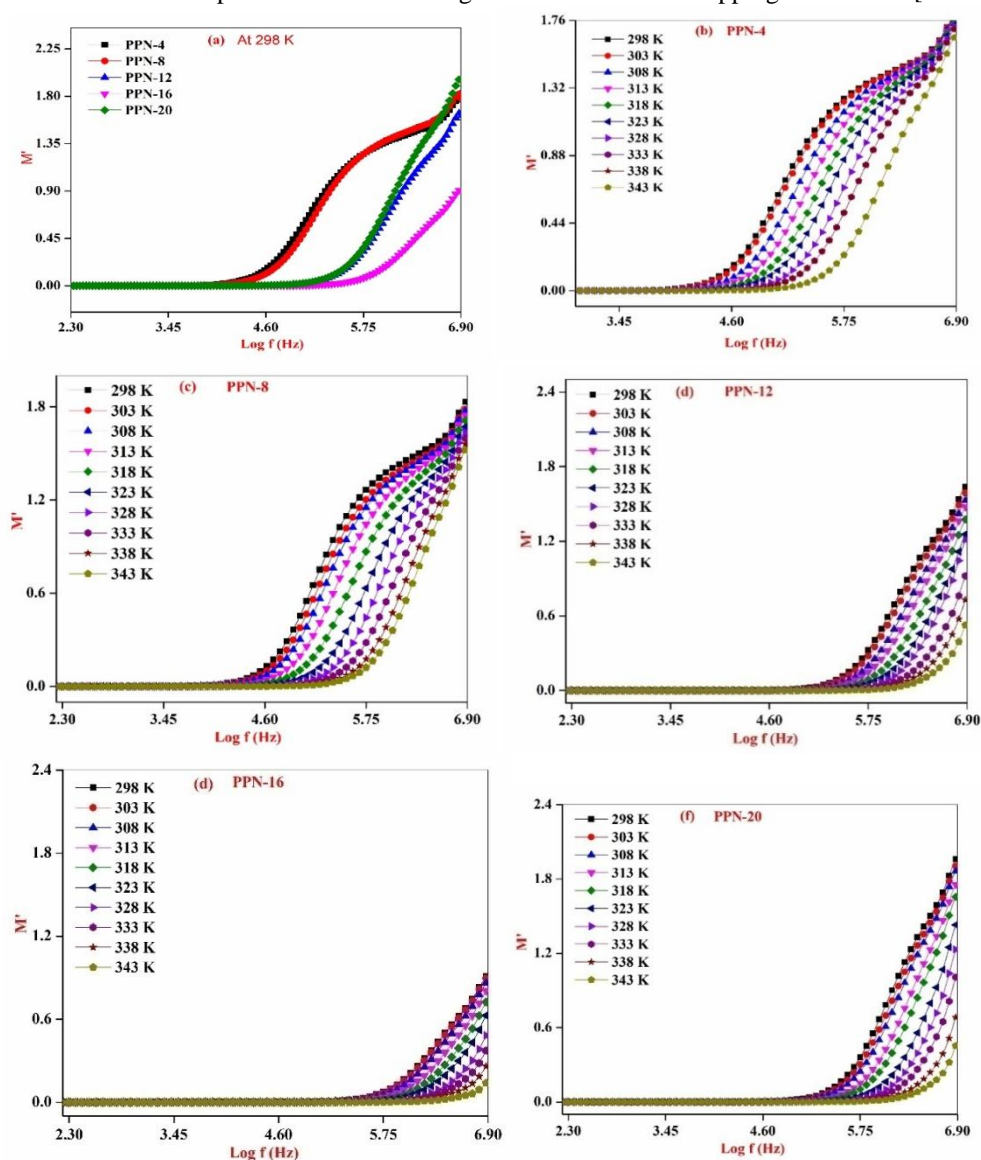


Fig. 3.4.1 Real electric modulus varies with frequency of several blend polymer electrolytes: (a) at 298 K and (b to f) at different temperatures.

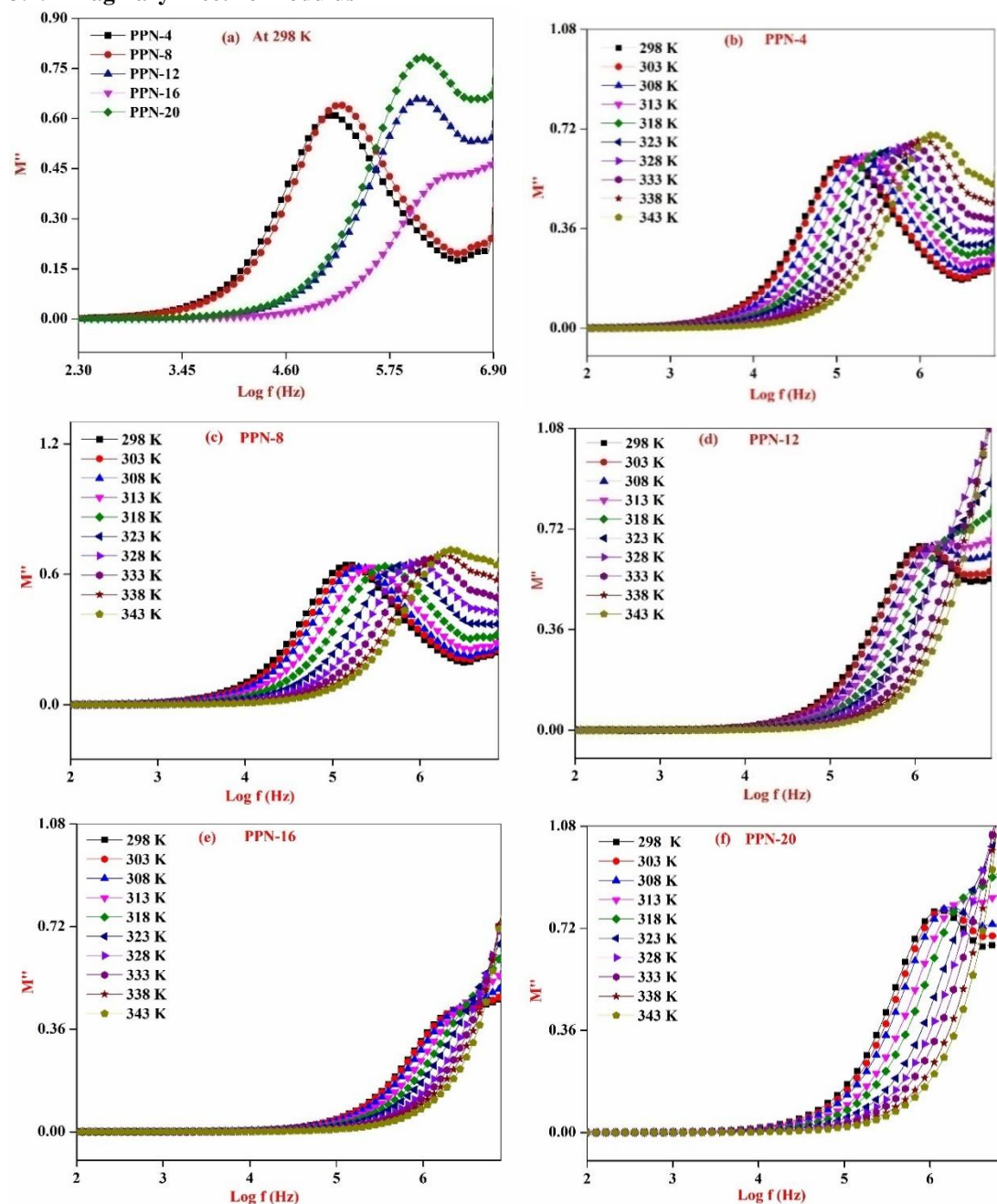
3.4.2 Imaginary Electric Modulus

Fig. 3.4.2 Imaginary electric modulus varies with frequency of several blend polymerelectrolytes: (a) at 298 K and (b to f) at different temperatures

Figure 3.4.2 (a) displays the frequency dependence of the imaginary electric modulus (M'') for altogether PPN electrolyte systems measured at 298K. In the lower frequency region, the imaginary portion of the "modulus" approaches value of zero, due to electrode interface polarization is quite small. The imaginary electric modulus values rise with frequency and attain highest values at the frequency of resonance (f_r) and observed as a shift towards higher frequencies with increasing temperature. This could be due to quick charge carrier movement, relaxation time may be shortened [14, 15]. The process of relaxation of ions in Polymer electrolyte systems can be described by the imaginary modulus peaks spectra at greater frequencies, these were noticed to be greatest for the PPN-16 electrolyte system. The temperature dependence of M'' for the PPN-4, PPN-8, PPN-12, PPN-16, and PPN-20 systems is shown in Figs. 3.4.2 (b-f). The non-Debye behaviour of the material is responsible for the asymmetric peaks in the M'' spectrum.

Conclusions

The salt concentration has been varied with fixed blend composition (i.e. 80 wt% PVP: 20 wt% PVDF: x wt% NaClO₄, where x= 4, 8, 12, 16, and 20). In this system, the ionic conductivity increases with salt concentration up to 16wt%, further decreases. The highest ionic conductivity has been noticed 9.334×10^{-5} S/cm for 80 wt% PVP: 20 wt% PVDF: 16 wt% NaClO₄

Acknowledgement

The authors are appreciative to the head of the physics department at Osmania University in Hyderabad and to DST PURSE-II for their kind assistance and the use of their experimental facilities.

Conflicts of Interest

The authors certify that they do not have any competing interests to declare.

References

- [1]. Mohanty, Hari Sankar, Ashok Kumar, Pawan K. Kulriya, Reji Thomas, and Dillip K. Pradhan. Materials Chemistry and Physics, 230 (2019) 221-230.
- [2]. T. Sreekanth, M. Jaipal Reddy, S. Rama Lingaiah, U.V. Subba Rao. Journal of power sources, 79 (1999) 105-110.
- [3]. Xiaomei Cai, Tingping Lei, Daoheng Sun and Liwei Lin. RSC Advances, 7 (2017) 15382-15389.
- [4]. Shobhna Choudhary, R. J. Sengwa. Electrochemical Acta, 247 (2017) 924-941.
- [5]. Jingyu Xi, Xinping Qiu, Mengzhong Cui, Xiaozhen Tang, Wentao Zhu, Liquan Chen. Journal of Power Sources, 156 (2005) 581–588.
- [6]. Zhaohui Li, Guangyao Su, Xiayu Wang, Deshu Gao. Solid State Ionics, 176 (2005) 1903-1908.
- [7]. S. Das, A. Ghosh. Journal of Applied Physics, 119 (2016) 095101.
- [8]. Yalla Mallaiah, Venkata Ramana Jeedi, R. Swarnalatha, A. Raju, S. Narender Reddy, A. Sadananda Chary. J. Phy and Che Solids, 155 (2021) 110096
- [9]. Praveen, D., S. V. Bhat, and Ramakrishna Damle. Ionics, 19(10) (2013) 1375-1379.
- [10]. S. Rajendran, M. Sivakumar, R. Subadevi. J. Power Sources, 124 (2003) 225–230.
- [11]. X.H. Flora, M. Ulaganathan, S. Rajendran. Int. J. Electrochem. Sci, 7 (2012) 7451–7462.
- [12]. S. Choudhary, R.J. Sengwa. Curr. Appl. Phys, 18 (2018) 1041–1058
- [13]. G.N. Mathioudakis, A.C. Patsidis, G.C. Psarras. J. Therm. Anal. Calorim, 116 (2014) 27–
- [14]. Aziz SB, Abidin ZHZ, Arof AK. Express Polym Lett, 4 (2010) 300–310.
- [15]. Dutta A, Sinha TP, Jena P, Adak S. J Non-Cryst Solids, 354 (2008) 3952–3957.